electronic reprint

Journal of
Applied Crystallography
ISSN 0021-8898
Editor: **Gernot Kostorz**

On the sensitivity of electron and X-ray scattering factors to valence charge distributions

Jin-Cheng Zheng, Yimei Zhu, Lijun Wu and James W. Davenport

Copyright © International Union of Crystallography

Author(s) of this paper may load this reprint on their own web site provided that this cover page is retained. Republication of this article or its storage in electronic databases or the like is not permitted without prior permission in writing from the IUCr.

Journal of
Applied Crystallography
ISSN 0021-8898

Received 11 January 2005
Accepted 19 May 2005

On the sensitivity of electron and X-ray scattering factors to valence charge distributions

Jin-Cheng Zheng, Yimei Zhu,* Lijun Wu and James W. Davenport

Brookhaven National Laboratory, Upton, NY 11973, USA. Correspondence e-mail: zhu@bnl.gov

The sensitivity of atomic scattering factors to valence charge distributions has been compared quantitatively for X-ray and electron diffraction. It is found that below a critical scattering vector, **s** ($|\mathbf{s}| = \sin\theta/\lambda$), ranging typically from 0.2 to 0.6 Å^{-1} depending on the atomic number, electron diffraction is more sensitive to valence charge densities than X-ray diffraction. Thus, electron diffraction provides crucial electronic structure information *via* the low-order structure factors, which are relatively insensitive to thermal vibrations, but sensitive to the charge distribution that characterizes the chemical bonding properties of the materials. On the other hand, the high-order structure factors, which are mainly influenced by atomic position and core charge, in many cases can be replaced by structure factors of a procrystal (superposition of neutral atoms), or by calculated structure factors from modern density functional theory (DFT), without losing significant accuracy. This is demonstrated by detailed analyses of an MgB_2 superconductor. The work reveals the importance of accurate determination of a very few low-order structure factors in valence electron density studies, and suggests the merit of the combined use of electron diffraction and DFT calculations for solids, especially those with large unit cells and nanocrystalline grains, unsuitable for X-ray studies.

© 2005 International Union of Crystallography
Printed in Great Britain – all rights reserved

1. Introduction

The experimental charge density in materials can be measured using two complementary techniques: X-ray and electron diffraction. X-ray diffraction (XRD) measures the total density of electrons in solids from the X-ray structure factors, which are the Fourier components of the electron density, while electron diffraction (ED) measures electron structure factors, the Fourier components of the electrostatic potential. Electron structure factors can be converted to X-ray structure factors using the Mott formula (Mott & Massey, 1965). Structure factors at small scattering vector **s** ($|\mathbf{s}| = s = \sin\theta/\lambda$, where θ is the scattering angle and λ is the wavelength of incident electrons or X-rays) are difficult to measure accurately with X-ray diffraction in single-crystal experiments because of extinction, or by powder diffraction experiments (polycrystals with small grains). On the other hand, in a transmission electron microscope (TEM), a very small electron probe can be used to study a defect-free nanometre region in the sample owing to the strong interaction between the incident electrons and the sample, although quantitative analysis has been a challenge. The recent development of quantitative electron diffraction using a convergent electron beam, such as convergent beam electron diffraction (CBED) (Zuo, 1993, 1999; Zuo, O'Keeffe *et al.*, 1997; Zuo, Blaha & Schwarz, 1997) and parallel recording of dark-field images (PARODI) (Taftø *et al.*, 1998; Zhu & Taftø, 1997; Zhu *et al.*, 2003; Wu *et al.*, 2004) has opened the door to mapping valence electron distributions by accurately determining the structure factors of the innermost reflections. With CBED, we record electron diffraction from a sample with a consistent thickness, which is relatively straightforward and suitable for small unit cells. With PARODI, we analyze intensity oscillations of image-coupled diffraction patterns from a sample with varying thickness. The latter technique is more complex due to the thickness involved; nevertheless, it does not require a larger convergent-beam angle, and can be used for crystals with large unit cells. The disadvantage of electron diffraction is that the analysis is often time consuming, largely due to the dynamic scattering effects, and thus, in contrast to X-rays, it is not suitable for the measurement of a large number of reflections, especially the high-order reflections, due to the poor signal/noise ratio. Because of their complementarity, it seems important to compare the advantages and drawbacks of the electron and X-ray diffraction techniques in the study of charge distributions.

Charge densities may also be obtained theoretically using first-principles calculations based on density functional theory (DFT) (Hohenberg & Kohn, 1964; Kohn & Sham, 1965; Parr & Yang, 1989). These are usually carried out with full potential (all electron) methods that fully take into account the contributions from both valence and core electrons (see, for example, Wu *et al.*, 2004; Lu *et al.*, 1993, 1995). In principle, there is no limitation of access to materials by DFT methods. The accuracy of structure factors calculated by DFT does rely on the approximations to exchange and correlation potentials,

electronic reprint

as well as the convergence control in the program. However, recent results have been quite accurate, so that, basically, DFT calculations can be regarded as an independent, complementary probe for charge density and structure factors, comparable with ED and XRD.

Electron diffraction is very sensitive to valence electron distribution compared with X-ray diffraction, as suggested by the Mott formula (Mott & Massey, 1965): $f_{el}(s) \propto (1/s^2)/[Z - f_x(s)]$ where $f_{el}(s)$ and $f_x(s)$ are the atomic scattering amplitudes for electron diffraction and X-ray diffraction, respectively, **s** is the scattering vector (magnitude s), and Z is the charge of the nucleus.

The basic reason for the sensitivity is the near cancellation of the scattering from the positively charged nucleus and the negatively charged electrons. Thus small changes in electron density lead to large changes in the scattering. The well known divergence at small s for Coulomb scattering helps to overcome the near cancellation and leads to strong measurable scattered intensities. However, the quantitative evaluation of the contribution of electron and X-ray scattering factors to charge distributions as a function of scattering angle is not well established. In this paper, we describe the sensitivity of electron and X-ray scattering factors to charge distributions, and the sensitivity of charge rearrangement, thermal vibrations and orbital electrons as a function of scattering vector. A possible approach to the analysis of charge density is proposed, and the merits of the combined use of electron diffraction measurements and DFT calculations are also discussed.

2. The sensitivity of scattering factors to charge distributions: X-rays *versus* electrons

2.1. Atomic case: form factor

The X-ray form factors can be expressed as a Fourier transform of charge density (Rez *et al.*, 1994; Hahn, 2002):

$$f_x(s) = 4\pi \int_0^\infty r^2 \rho(r)[\sin(4\pi sr)/(4\pi sr)]\,\mathrm{d}r, \tag{1}$$

where $s = \sin\theta/\lambda$. The X-ray scattering factors are often parameterized as a sum of some Gaussians (Rez *et al.*, 1994),

$$f_x(s) = \sum_j a_j \exp(-b_j s^2), \tag{2}$$

where a_j and b_j are fitting parameters. The electron form factors can be obtained from the Mott formula (Mott & Massey, 1965; Spence & Zuo, 1992; Peng, 1997),

$$f_{el}(s) = \frac{|e|}{16\pi^2 \varepsilon_0 s^2}[Z - f_x(s)]. \tag{3}$$

We can express the comparison of sensitivity between X-ray and electron form factors in the following way:

$$\frac{\zeta_{el}(s)}{\zeta_x(s)} = -\frac{f_x(s)}{[Z - f_x(s)]}, \tag{4}$$

where $\zeta_x(s) = \mathrm{d}f_x(s)/f_x(s)$ and $\zeta_{el}(s) = \mathrm{d}f_{el}(s)/f_{el}(s) = [1/f_{el}(s)][\partial f_{el}(s)/\partial f_x(s)]\mathrm{d}f_x(s)$ are the sensitivity of the X-ray and electron form factors as a function of the scattering vectors, respectively; and $\mathrm{d}f_x(s)$ and $\mathrm{d}f_{el}(s)$ are the variation of the X-ray and electron form factors. Fig. 1 shows the behavior of equation (4) as a function of s, taking Cu as the example.

It is interesting to see in what region of the scattering vectors the sensitivity of electron scattering factors is superior to that of X-ray scattering factors. This can be obtained from equation (4) together with a critical condition:

$$\left|\zeta_{el}(s)/\zeta_x(s)\right| > 1. \tag{5}$$

Thus

$$f_x(s) > Z/2. \tag{6}$$

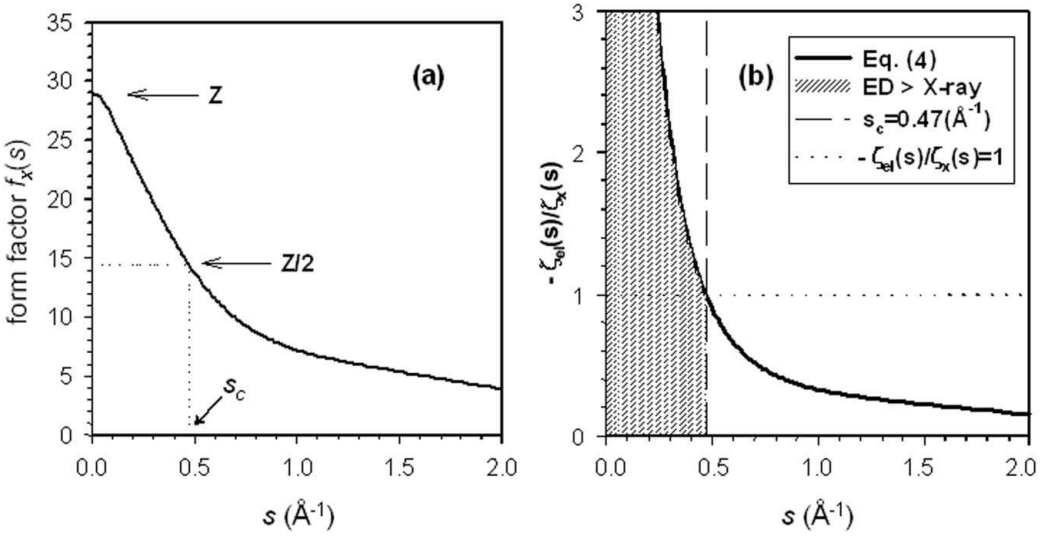

Figure 1
(*a*) X-ray form factors $f_x(s)$ and (*b*) the ratio of $-\zeta_{el}(s)/\zeta_x(s)$ as a function of scattering vector, s (Å^{-1}). The parameterized $f_x(s)$ data are from Su & Coppens (1997). The dotted line in (*b*) indicates where the sensitivities of ED and XRD are identical, and the dashed line shows the position of the critical scattering vector (s_c = 0.47 Å^{-1}). The shaded area marks the range of scattering vectors where ED is more sensitive than XRD to the valence charge distribution.

electronic reprint

The physical meaning of equation (6) is that in the scattering angle regime where X-ray scattering factors fulfill the condition of equation (6), electrons are more sensitive to the rearrangement of charge than X-rays. This mainly applies to low-order scattering factors. Therefore, the critical scattering vectors, s_c, can be determined from

$$f_x(s_c) = Z/2 \tag{7a}$$

or

$$f_{el}(s_c) = \frac{|e|}{16\pi^2\varepsilon_0 s_c^2}\frac{Z}{2}. \tag{7b}$$

If the X-ray scattering factors are parameterized as a sum of some Gaussians as expressed in equation (2), the critical scattering vectors (s_c) can be determined from

$$\sum_j a_j \exp(-b_j s_c^2) = \frac{Z}{2}. \tag{8}$$

In practice, the critical scattering vectors (s_c) can be obtained from standard tables of X-ray scattering factors for atoms (or ions) (Rez *et al.*, 1994), or from the numerical solution of equation (8).

Fig. 2 gives the calculated critical scattering vectors for atoms from H to Xe. For light elements, these vectors range from 0.2 to 0.4 Å^{-1}, while, for heavy elements, they are around 0.5 to 0.6 Å^{-1}.

2.2. Crystal case: structure factor

The electron structure factor is given by the Mott–Bethe expression (Coppens, 1997):

$$F_{el}(\mathbf{s}) = \frac{|e|}{16\pi^2\varepsilon_0 V_{\text{unit cell}}} \times \sum_i \frac{[Z_i - f_{x_i}(s)]}{s^2}\exp(-B_i s^2)\exp(4\pi i\mathbf{s}\cdot\mathbf{r}_i), \tag{9}$$

and the X-ray structure factor can be written as

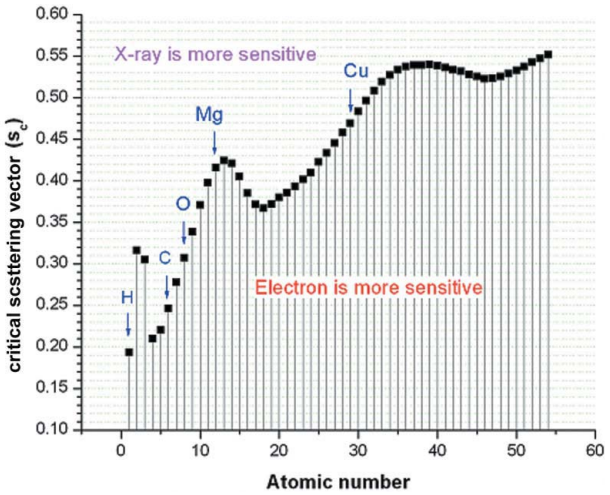

Figure 2
The critical scattering vector s_c for the atoms H to Xe.

$$F_x(\mathbf{s}) = \sum_i f_{x_i}(s)\exp(-B_i s^2)\exp(4\pi i\mathbf{s}\cdot\mathbf{r}_i) \tag{10}$$

where $f_{x_i}(s)$ is the ith atomic X-ray form factor, and B_i is the Debye–Waller factor that characterizes the temperature factor. Similar to the form-factor case, the critical scattering vector ($\mathbf{s}_c$) of the structure factor can be determined by

$$\left|\sum_i [f_{x_i}(s_c) - Z_i/2]\exp(-B_i s_c^2)\exp(4\pi i\mathbf{s}_c\cdot\mathbf{r}_i)\right| \to 0, \tag{11a}$$

or in terms of structure factors F_x,

$$\left|F_x(s_c) - \sum_i (Z_i/2)\exp(-B_i s_c^2)\exp(4\pi i\mathbf{s}_c\cdot\mathbf{r}_i)\right| \to 0. \tag{11b}$$

Here, we use $\to$ instead of = in equations (11) because the scattering vector is discrete in the case of the crystal structure factor. Equation (11) suggests that the critical scattering vector $\mathbf{s}_c$ is structure and temperature dependent. For B_i = constant, the Debye–Waller factors are the same for all atoms in the unit cell and equation (11a) can be simplified as

$$\left|\sum_i [f_{x_i}(s_c) - Z_i/2]\exp(4\pi i\mathbf{s}_c\cdot\mathbf{r}_i)\right| \to 0. \tag{12}$$

For the monatomic case, $f_{x_i}(\mathbf{s}_c) = f_x(\mathbf{s}_c)$, and $Z_i = Z$, equation (12) becomes

$$f_x(\mathbf{s}_c) \to Z/2. \tag{13}$$

The critical scattering vector $\mathbf{s}_c$ of the structure factor determined by equation (13) is similar to the critical scattering vector of the form factor. For example, the critical scattering vector of the structure factor for Si is $s_c \simeq 0.4$ Å^{-1}, similar to that of its form factor. For polyatomic crystals, the critical scattering vector of the structure factor is related to the detailed arrangement of the unit cell (atomic coordinates). Here, we use MgB_2 as an example to examine the critical scattering vector.

In the independent-atom model (considering free atoms before interatomic bonding, hereafter denoted as IAM), the structure factor of MgB_2 can be expressed as

$$\begin{aligned} F^{hkl} &= \sum_i f_i(s)\exp(4\pi i\mathbf{s}\cdot\mathbf{r}_i) \\ &= f_{Mg}^{hkl} + f_B^{hkl}\left\{\exp\left[i2\pi\left(\tfrac{1}{3}h + \tfrac{2}{3}k + \tfrac{1}{2}l\right)\right]\right. \\ &\quad \left. + \exp\left[i2\pi\left(\tfrac{2}{3}h + \tfrac{1}{3}k + \tfrac{1}{2}l\right)\right]\right\}, \end{aligned} \tag{14}$$

where f_{Mg}^{hkl} and f_B^{hkl} are the form factors of Mg and B, respectively. The formula related to the $Z_i/2$ term is

$$\begin{aligned} \sum_i (Z_i/2)\exp(4\pi i\mathbf{s}_c\cdot\mathbf{r}_i) &= \tfrac{1}{2}Z_{Mg} + \tfrac{1}{2}Z_B\left\{\exp\left[i2\pi\left(\tfrac{1}{3}h + \tfrac{2}{3}k + \tfrac{1}{2}l\right)\right]\right. \\ &\quad \left. + \exp\left[i2\pi\left(\tfrac{2}{3}h + \tfrac{1}{3}k + \tfrac{1}{2}l\right)\right]\right\} \\ &= 6 + 2.5\left\{\exp\left[i2\pi\left(\tfrac{1}{3}h + \tfrac{2}{3}k + \tfrac{1}{2}l\right)\right]\right. \\ &\quad \left. + \exp\left[i2\pi\left(\tfrac{2}{3}h + \tfrac{1}{3}k + \tfrac{1}{2}l\right)\right]\right\}. \end{aligned} \tag{15}$$

Fig. 3 plots the X-ray structure factors of MgB_2 calculated from the DFT and IAM models, and with the above $Z_i/2$ term. It shows that DFT and IAM values are larger than the $Z_i/2$

electronic reprint

values in the range of $s < 0.3$ Å^{-1} (indicated by the arrow I), and smaller in the range of $s > 0.6$ Å^{-1} (indicated by the arrow II). Over 0.3 Å^{-1} $< s <$ 0.6 Å^{-1}, some calculated structure factors are larger and others are smaller than the $Z_i/2$ term. We note that the critical scattering vector for the B form factor is 0.22 Å^{-1} and the value for Mg is 0.42 Å^{-1}. For a polyatomic crystal with various s_c for different atomic species, say ranging from s_c^{min} to s_c^{max}, an estimate can be made, although strictly speaking they are very much crystal symmetry dependent. In general, for $s < s_c^{min}$, ED is more sensitive, and for $s > s_c^{max}$, XRD is more sensitive. Over $s_c^{min} < s < s_c^{max}$, the sensitivity depends on the particular reflection.

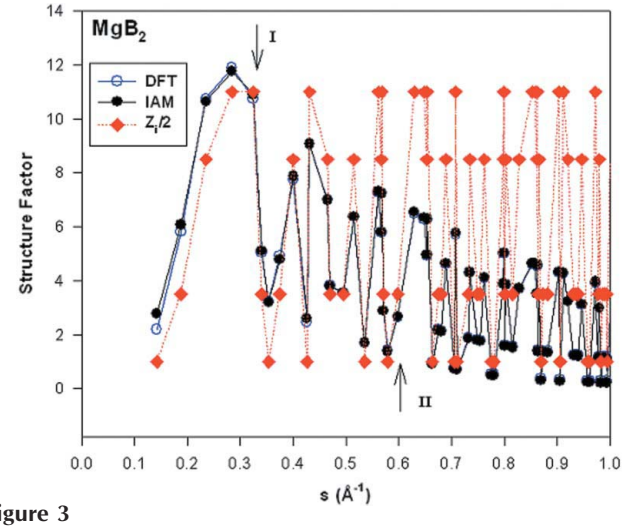

Figure 3
The structure factors of MgB_2 calculated from DFT and IAM models, as well as those from the $Zi/2$ term [using equation (15)] as a function of scattering vector, s.

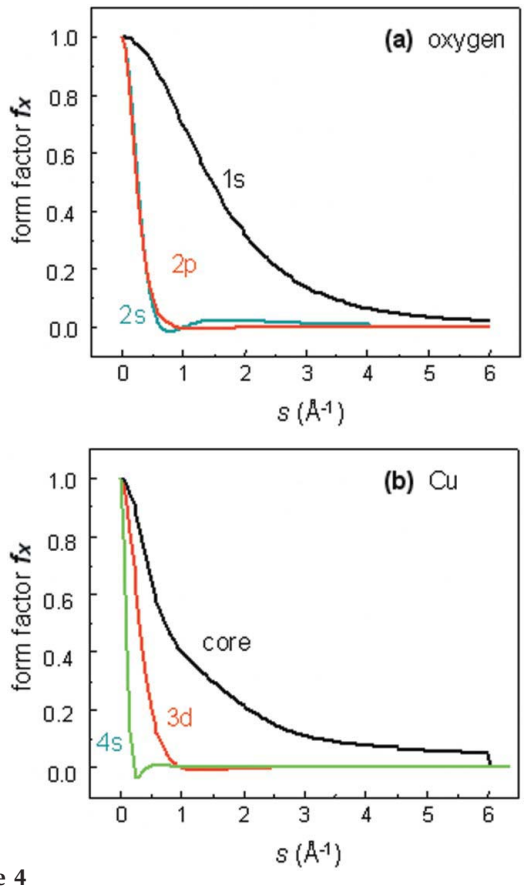

Figure 4
X-ray scattering amplitude $f_x(s)$ of core and valence electrons for (*a*) O and (*b*) Cu (data from Su & Coppens, 1997) normalized to one electron.

3. The sensitivity of scattering factors to charge distributions: low-order *versus* high-order reflections

3.1. Atomic case: form factor

Since the core electrons are close to the nuclei while the valence electrons are outer electrons, scattering by the core electrons could extend to large s, while that by the valence electrons will mostly be concentrated at small s. Fig. 4 clearly shows the difference in scattering amplitude for core and valence electrons of oxygen and copper. In general, the f_x for core electrons decreases smoothly with increasing s. By contrast, the f_x for valence electrons drops fast with s, and closes to zero at $s > 1$. When atoms form a crystal, the arrangement of their valence electrons generally changes, while the core electrons do not. Therefore, there may be a significant difference between the low-order reflections in a real crystal and in a procrystal (a hypothetical crystal with atoms having the electron distribution of free atoms), but a negligible difference in the high-order reflections.

3.2. Crystal case: structure-factor difference between the crystal and procrystal

To verify the effects of low-order structure factors on analyses of charge density, the following two factors can be assessed: (*a*) structure-factor difference between the crystal and procrystal as a function of the scattering vector; and (*b*) the response of charge density and bonding properties to variations in low-order and high-order structure factors: *i.e.* charge density, the gradient, Laplacian of charge density, and electric field gradient (EFG). Factor (*a*) basically provides information on the impact factor (or percentage of contributions) from low-order structure factors compared with high-order structure factors. Factor (*b*) is related to the sensitivity of variation in low-order structure factors to total charge distribution and bonding properties. We describe these two factors next.

In a hypothetical crystal, either a procrystal or IAM, the spherical electron densities of atoms overlap. The difference in charge densities between the real crystal $\rho_c(\mathbf{r})$ and the procrystal $\rho_p(\mathbf{r})$ is the so-called deformation density, also referred to as the difference charge density, and defined as

$$\Delta\rho(\mathbf{r}) = \rho_c(\mathbf{r}) - \rho_p(\mathbf{r}). \qquad (16)$$

This deformation density characterizes the rearrangement of charge distribution, especially the valence charge density, as well as the bonding properties. Deformation density is a key feature in describing charge distribution in crystals in diffraction studies. The Fourier components of deformation density are difference structure factors, *i.e.* the difference

electronic reprint

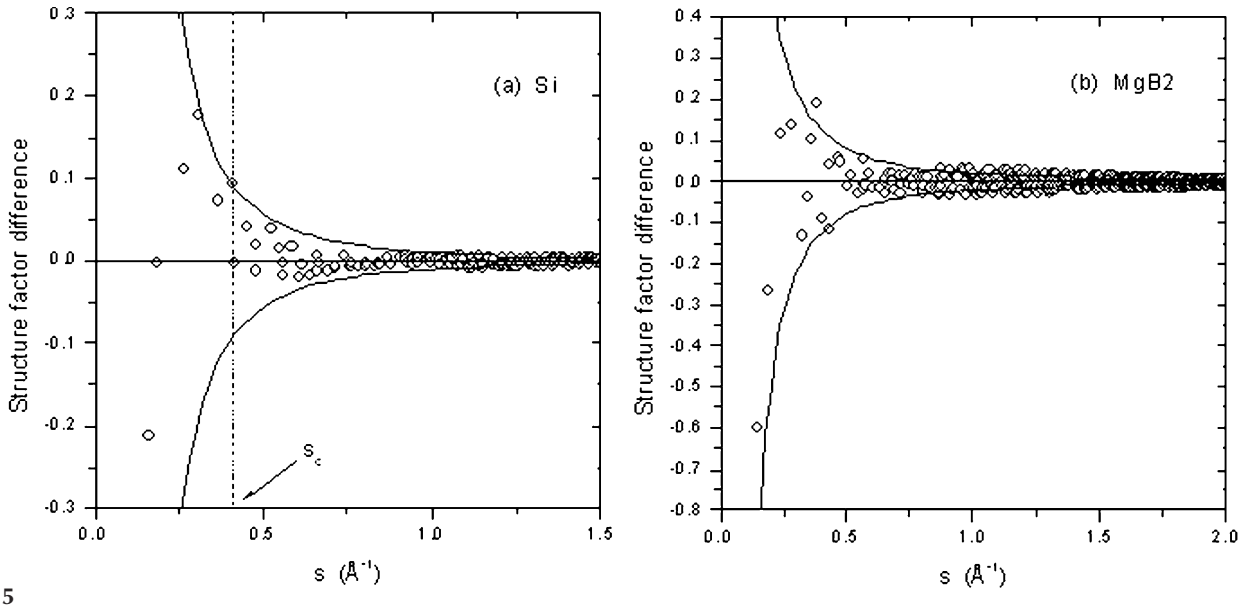

Figure 5
Difference in the X-ray structure factors between the crystal and neutral atom (procrystal) of (*a*) Si and (*b*) MgB_2 calculated by DFT using FPAPW (GGA). The thin lines are plotted using $\pm as^{-b}$, with $a = 0.01$ and $b = 2.5$ for Si, and $a = 0.02$, $b = 2.0$ for MgB_2. The critical scattering vector for Si, $s_c \simeq 0.4$ Å^{-1}, is also indicated.

between real crystal structure factors $F_c(\mathbf{s})$ and structure factors from the procrystal $F_p(\mathbf{s})$. Therefore, the difference structure factors $\Delta F(\mathbf{s}) = F_c(\mathbf{s}) - F_p(\mathbf{s})$ as a function of s will provide information on valence charge distribution and charge transfer:

$$\Delta\rho(\mathbf{r}) = \frac{1}{V}\sum_s \Delta F_x(\mathbf{s}) \exp(-4\pi i \mathbf{s}\cdot\mathbf{r}), \qquad (17)$$

where V is the volume of the unit cell.

Fig. 5 plots the difference of X-ray structure factors (between crystal and procrystal) for Si (covalent bonding) and MgB_2 (mixture of ionic and covalent). It shows that only very few low-order structure factors (with $s < 0.5$ Å^{-1}, indicated by the dotted line in Fig. 5) are significantly different from those of the procrystal, and they provide the main contributions to the valence charge distribution. Especially, the fact that the first two structure factors in MgB_2 have large differences from procrystal suggest that small changes in these structure factors will lead to marked modifications in the difference charge density and, thus, the bonding properties.

3.3. Case studies

The sensitivity of charge density and bonding properties to variations in different-order structure factors can be judged from equation (17). As Fig. 5 shows, ΔF decreases with increases in s and approaches zero at large s. We note that this behavior of ΔF is found in many solid crystals and is not limited to Si and MgB_2. We also find that ΔF often exhibits a trend that can be expressed approximately as a function of $\pm as^{-b}$, where a and b are positive material-dependent parameters (Fig. 5). Therefore, the contributions from different structure factors will have a similar factor of as^{-b}. In other words, the main contributions to the valence electron distribution (related to chemical bonding) are dominant in low-order structure factors.

To justify further the importance of low-order structure factors in charge density analysis, we examined the sensitivity of charge density to a wide range of structure factors in MgB_2. We verified the findings by checking the changes of charge density ρ, the gradient $\nabla\rho$ and Laplacian $-\nabla^2\rho$ of charge density, and EFG as a function of the variation of ten structure factors with s ranging from 0.1 to 2.6 Å^{-1}. All the structure factors in this examination are from DFT calculations using the generalized gradient approximation (GGA) function parameterized by Engel & Vosko (1993). The structure factor of each low-order reflection was varied from −10% to 10%, while the other 5777 structure factors remained at their original values (*i.e.* from DFT calculations). Our calculations revealed that a very small variation in a single low-order structure factor always leads to large changes in charge density, Laplacian and EFG, while for high-order structure factors, such changes are very small and can be neglected, as shown in detail in Fig. 6.

3.4. Temperature effects

The Debye–Waller factor B characterizes the effects of temperature (lattice vibrational effects) in the calculations of structure factors and the analysis of charge density. In this section, we analyze the sensitivity of different-order (low and high) structure factors to variations in the Debye–Waller factor B. The structure factor at finite temperature can be expressed as

$$F_T = F_0 \exp(-Bs^2), \qquad (18)$$

where F_0 is the structure factor at 0 K and B is the Debye–Waller factor at temperature T. If the temperature changes by ΔT, the Debye–Waller factor will change accordingly, *i.e.* ΔB.

electronic reprint

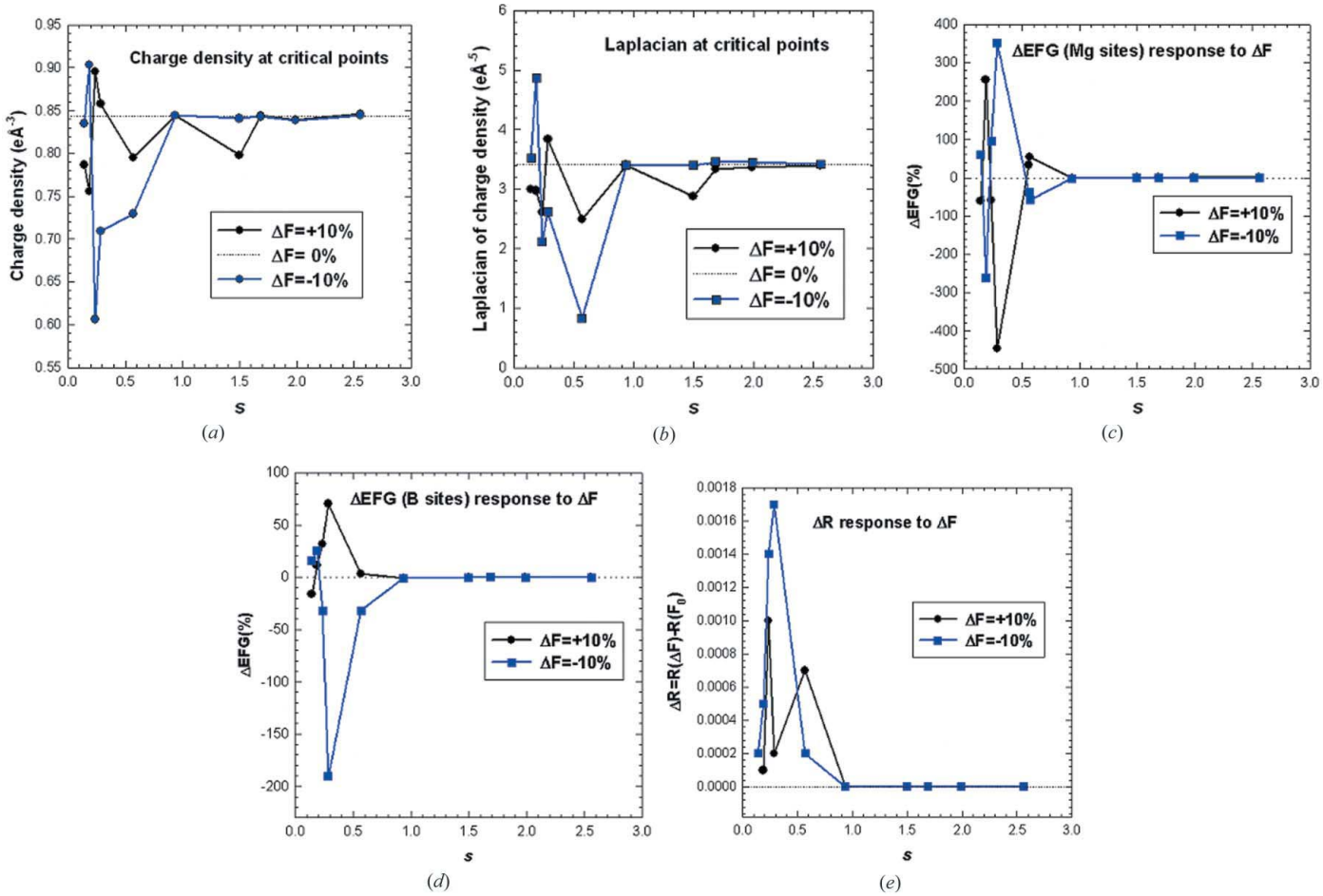

Figure 6
Sensitivities as a function of scattering vector s by examining $\pm 10\%$ changes of the structure factors ΔF of the ten reflections (001, 100, 101, 002, 300, 004, 500, 800, 900, 0014 and 0018) in MgB_2. Sensitivity to: (*a*) the charge density, ρ, (*b*) the Laplacian of the charge density, $-\nabla^2\rho$, at the critical point ($\nabla\rho = 0$) [the middle point of the B–B bond in the (001) boron plane], (*c*,*d*) the change of electric field gradient, ΔEFG, at Mg (*c*) and B (*d*) sites, and (*e*) the corresponding difference of R factors: $\Delta R = R(\Delta F) - R(F_0)$, where $R(\Delta F)$ is the goodness of fit after the change of structure factors, and $R(F_0)$ is before the change of structure factors.

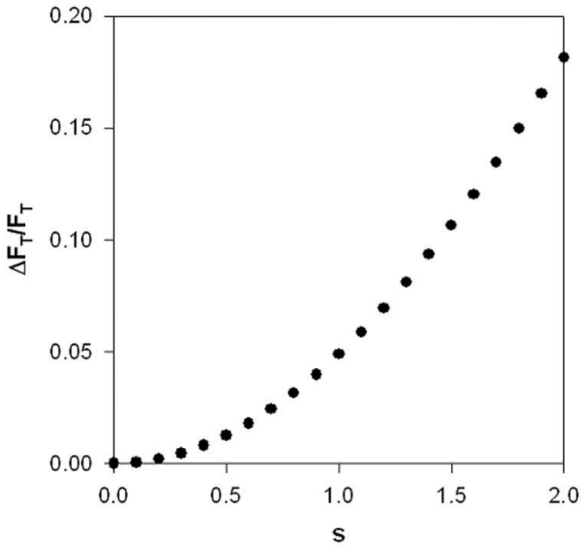

Figure 7
$\Delta F_T/F_T$ as a function of scattering vector s with $\Delta B = 0.05$.

The related change of the structure factor ΔF_T can be obtained as

$$\Delta F_T = F_T[1 - \exp(-\Delta B s^2)]. \quad (19)$$

In Fig. 7, $\Delta F_T/F_T$ is plotted as a function of s with $\Delta B = 0.05$. It demonstrates that the variation of low-order structure factors is not as sensitive as that of high-order structure factors to the variation in the Debye–Waller factor. This indicates that for the study of valence charge distribution, it is not crucial to determine the atomic positions accurately, especially due to the small change of temperature. In contrast, the core charge is very sensitive to thermal vibrations.

3.5. Combined use of electron diffraction measurements and DFT calculations

Since the bonding properties are mainly determined by the deformation of charge density, which can be analyzed by topological features, they are encoded unambiguously in the low-order structure factors. This is exciting to researchers

electronic reprint

Table 1
Comparison of low-order structure factors obtained from electron diffraction (ED) at $T = 0$ K.

Data at 0 K were converted from those of Wu *et al.* (2004) at $T = 298$ K with Debye–Waller factor of $B = 0.4$. The calculations were based on DFT (GGA and LDA) and procrystal theory. Different models for GGA were used: EV (Engel & Vosko, 1993), PBE (Perdew *et al.*, 1996) and PW91 (Perdew & Wang, 1992). The R factors were defined as: $R1 = \sum[F_{(\mathrm{DFT})} - F_{(\mathrm{ED})}]/\sum F_{(\mathrm{ED})}$ and $R2 = \sum\{[F_{(\mathrm{DFT})} - F_{(\mathrm{ED})}]/F_{(\mathrm{ED})}\}$, where $F_{(\mathrm{DFT})}$ and $F_{(\mathrm{ED})}$ are structure factors from DFT and ED, respectively.

			DFT (GGA)				
	s (Å^{-1})	Measurement (ED)	EV	PBE	PW91	DFT (LDA)	Procrystal
0 0 1	0.142	2.17 ± 0.03	2.195	2.195	2.188	2.202	2.783
1 0 0	0.187	5.61 ± 0.07	5.793	5.798	5.793	5.803	6.077
1 0 1	0.235	10.88 ± 0.14	10.749	10.757	10.764	10.752	10.648
0 0 2	0.284	11.81 ± 0.17	11.866	11.892	11.904	11.890	11.760
$R1$ (%)			0.48	0.61	0.63	0.62	3.23
$R2$ (%)			3.92	4.31	4.05	4.67	41.42

because, although normally only a few innermost reflections are measurable with high accuracy using electron diffraction, nevertheless their structure factors are most sensitive to capture the information on valence charge distribution (namely, deformation density) and chemical bonding. On the other hand, the values of high-order structure factors are very close to those of the procrystal, which reflect mainly the charge density of independent (or free) atoms prior to forming chemical bonds. Therefore, it should be possible to obtain valuable data on charge density by analyzing a combination of accurate low-order structure factors measured with electron diffraction and high-order structure factors, which can be obtained from X-ray diffraction or DFT calculation, or even procrystal structure factors. It has been demonstrated (Zuo, O'Keeffe *et al.*, 1997) that the combination of some low-order structure factors assessed by electron diffraction with high-order structure factors from X-ray diffraction can yield accurate measurement of charge distributions in MgO. Based on our arguments above, it seems that it is not only possible but also valuable to combine electron diffraction and DFT calculations in charge density analysis in the cases where X-ray data are not available, for instance, in the case of high-temperature superconductors.

The deformation density $\Delta\rho_{\mathrm{mix}}(\mathbf{r})$ from the combination of structure factors obtained from different methods (labeled as subscript I and II) can be expressed as

$$\Delta\rho_{\mathrm{mix}}(\mathbf{r}) = \frac{1}{V}\sum_{s_{\mathrm{I}}} \Delta F_{\mathrm{x}}(s)\exp(-4\pi i\mathbf{s}\cdot\mathbf{r}) + \frac{1}{V}\sum_{s_{\mathrm{II}}} \Delta F_{\mathrm{x}}(s)\exp(-4\pi i\mathbf{s}\cdot\mathbf{r}). \quad (20)$$

This can be applied to X-ray, neutron and electron diffraction, and DFT calculations. For the combined use of electron diffraction (ED) and DFT calculations, we have

$$\rho_{\mathrm{mix}}(\mathbf{r}) = \rho_{\mathrm{DFT}}(\mathbf{r}) + \frac{1}{V}\sum_{\mathbf{s}} [F_{\mathrm{ED}}(s) - F_{\mathrm{DFT}}(s)]\exp(-4\pi i\mathbf{s}\cdot\mathbf{r}). \quad (21)$$

The deformation charge density can be obtained from the Fourier transformation of difference structure factors or can be reconstructed after multipole refinement (MR) (Coppens, 1997). The accuracy of this method is determined by the accuracy of the electron diffraction measurements, the DFT calculation and the multipole refinement. Quantitative electron diffraction, such as CBED (Zuo, O'Keeffe *et al.*, 1997; Zuo *et al.*, 1999) and PARODI (Taftø *et al.*, 1998; Zhu & Taftø, 1997; Zhu *et al.*, 2003), has demonstrated the possibility to measure the low-order structure factors with sufficient accuracy for charge density study. The accuracy of structure factors from DFT calculations can be controlled by employing self-consistent full-potential calculations (Blaha *et al.*, 2001) with advanced exchange-correlation potentials and treatment of strongly correlated interactions [such as local density approximation (LDA) with on-site Coulomb interaction (LDA + U), self-interaction corrections or dynamical mean field theory]. The charge density analysis of this ED + DFT method can be performed by direct Fourier summation (DF) or MR.

As an example, here we discuss the study of the charge density of MgB_2 by combining electron diffraction and DFT. Table 1 lists the four innermost low-order structure factors obtained from ED as well as those calculated from DFT with different approximations of the exchange-correlation potentials (Engel & Vosko, 1993; Perdew *et al.*, 1996; Perdew & Wang, 1992). As Table 1 shows, GGAs generally give closer values to ED than does the LDA. For the structure factors with the shortest reciprocal vectors (*i.e.* reflections 001 and 100), GGAs give smaller values compared with the LDA and agree better with the experimental data. Among the GGAs, the EV functional generates the most accurate values compared with the experimental data, as evidenced by the smallest R factors ($R1$ and $R2$, as defined in Table 1). This is very similar to the cases of Mg (Friis *et al.*, 2003) and Si (Zuo, Blaha & Schwarz, 1997) where the EV functional produced structure factors in close agreement with experimental values, due to its better description of core electrons.

Fourier summation and multipole refinements were performed for combined ED and DFT structure factors (*i.e.* the four low-order structure factors were replaced by experimental measurements). The EFGs calculated using combined ED and DFT structure factors are smaller than those using pure DFT structure factors from DF or MR. The EFGs calculated from combined ED and GGA-EV using MR are

electronic reprint

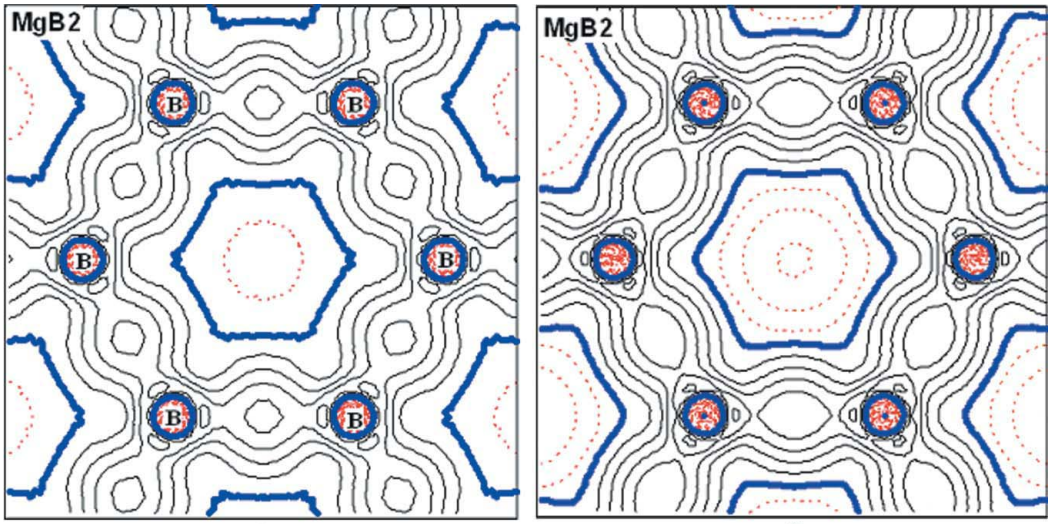

Figure 8
Difference charge density map of the (001) B plane in MgB_2: (*a*) from calculated structure factors based on direct Fourier summation of DFT (GGA-EV); and (*b*) modified difference map based on ED experiment and DFT. Note that the crucial low-order structure factors in (*a*) were replaced with the ED measurements in (*b*).

1.23 (10^{21} V m^{-2}) at B sites, and 0.20 (10^{21} V m^{-2}) at Mg sites, respectively, and are in good agreement with those estimated from X-ray diffraction (Tsirelson *et al.*, 2003): 1.25 (10^{21} V m^{-2}) at B sites and 0.21 (10^{21} V m^{-2}) at Mg sites, respectively. Although there are very few experimental structure factors (only four in this case), their effects on the valence electron distribution and EFG are substantial. Fig. 8 compares the difference map of charge density in MgB_2 obtained from all DFT-calculated structure factors (Fig. 8*a*) and the one corrected with electron diffraction measurements (Fig. 8*b*), *i.e.* combined ED-measured structure factors with DFT calculations. We note that although the difference between the ED measurements and the DFT is about a half percent, the difference between the procrystal and the DFT is only about 3% (see Table 1), suggesting that the minute deviation in structure factors at small s is still significant and cannot be overlooked. Clearly, with the four most sensitive low-order structure factors replaced by ED measurements, the maximum difference in charge density of a σ bond between the two boron atoms in the (001) B plane increases, indicating the enhanced covalent bonding between B atoms, which is considered to be responsible for the superconductivity of the material.

4. Conclusions

In conclusion, we have demonstrated that electron diffraction is more sensitive to valence electron distributions than X-ray diffraction at small scattering vectors ($s < s_c$ for monatomic cases and $s < s_c^{\min}$ for crystals). The low-order form factors and structure factors are extremely sensitive to small changes in the arrangement of valence electrons. These factors can be measured accurately using recently developed quantitative electron diffraction techniques, and also can be used to test DFT calculations, as demonstrated for the MgB_2 superconductor. Having verified the calculations, the calculated structure factors of high-order reflections may be combined with electron diffraction measurements of low-order reflections to understand valence electron distributions in materials. This approach is particularly useful when the X-ray diffraction data for a particular material are not available, or the material is not suitable for X-ray diffraction analysis.

The authors thank W. Ku for valuable discussions. This work was supported by the US Department of Energy, Division of Materials, Office of Basic Energy Science, under Contract No. DE-AC02-98CH10886.

References

Blaha, P., Schwarz, K., Madsen, G., Kvasnicka, D. & Luitz, J. (2001). *Wien2k*, *An Augmented Plane Wave + Local Orbitals Program for Calculating Crystal Properties* (Karlheinz Schwarz, Techn. Universitat Wien, Austria), ISBN 3-9501031-1-2.
Coppens, P. (1997). *X-ray Charge Densities and Chemical Bonding*. IUCr/Oxford University Press.
Engel, E. & Vosko, S. H. (1993). *Phys. Rev. B*, **47**, 13164–13174.
Friis, J., Madsen, G. K. H., Larsen, F. K., Jiang, B., Marthinsen, K. & Holmestad, R. (2003). *J. Chem. Phys.* **119**, 11359–11366.
Hahn, T. (2002). Editor. *International Tables for Crystallography*, Vol. A. Dordrecht: Kluwer.
Hohenberg, P. & Kohn, W. (1964). *Phys. Rev.* **136**, B864–B871.
Jiang, B., Zuo, J. M., Jiang, N., O'Keeffe, M. & Spence, J. C. H. (2003). *Acta Cryst.* A**59**, 341–350.
Kohn, W. & Sham, L. J. (1965). *Phys. Rev.* **140**, A1133–A1138.
Lu, Z. W., Zunger, A. & Deutsch, M. (1993). *Phys Rev B*, **47**, 9385–9410.
Lu, Z. W., Zunger, A. & Deutsch, M. (1995). *Phys. Rev. B.* **52**, 11904–11911.
Mott, N. F. & Massey, H. S. W. (1965). *The Theory of Atomic Collisions*. Oxford: Clarendon.
Parr, R. G. & Yang, W. T. (1989). *Density-Functional Theory of Atoms and Molecules*. Oxford University Press.
Peng, L. (1997). *Acta Cryst.* A**53**, 663–672.

electronic reprint

Perdew, J. P., Burke S. & Ernzerhof, M. (1996). *Phys. Rev. Lett.* **77**, 3865–3868.
Perdew, J. P. & Wang, Y. (1992). *Phys. Rev. B*, **45**, 13244–13249.
Rez, D., Rez, P. & Grant, I. (1994). *Acta Cryst.* A**50**, 481–497.
Spence, J. C. H. & Zuo, J. M. (1992). *Electron Microdiffraction*. New York: Plenum Press.
Su, Z. & Coppens, P. (1997). *Acta Cryst.* A**53**, 749–762.
Taftø, J., Zhu, Y. & Wu, L. (1998). *Acta Cryst.* A**54**, 532–542.
Tsirelson, V., Stash, A., Kohout, M., Rosner, H., Mori, H., Sato, S., Lee, S., Yamamoto, A., Tajima, S. & Grin, Yu. (2003). *Acta Cryst.* B**59**, 575–583.
Wu, L., Zhu, Y., Vogt, T., Su, H. & Davenport, J. W. (2004). *Phys. Rev. B*, **69**, 064501.
Zhu, Y. & Taftø, J. (1997). *Philos. Mag. B*, **75**, 785–791.
Zhu, Y., Wu, L. & Taftø, J. (2003). *Microsc. Microanal.* **9**, 442–456.
Zuo, J. M. (1993). *Acta Cryst.* A**49**, 429–435.
Zuo, J. M., Blaha, P. & Schwarz, K. (1997). *J. Phys. Condens. Matter*, **9**, 7541–7561.
Zuo, J. M., Kim, M., O'Keeffe, M. & Spence, J. C. H. (1999). *Nature (London)*, **401**, 49–52.
Zuo, J. M., O'Keeffe, M., Rez, P. & Spence, J. C. H. (1997). *Phys. Rev. Lett.* **78**, 4777–4780.

electronic reprint